

# Super-resolution 3D microscopy of live whole cells using structured illumination

Lin Shao<sup>1</sup>, Peter Kner<sup>2</sup>, E Hesper Rego<sup>1,3</sup> & Mats G L Gustafsson<sup>1,4</sup>

**Three-dimensional (3D) structured-illumination microscopy (SIM) can double the lateral and axial resolution of a wide-field fluorescence microscope but has been too slow for live imaging. Here we apply 3D SIM to living samples and record whole cells at up to 5 s per volume for >50 time points with 120-nm lateral and 360-nm axial resolution. We demonstrate the technique by imaging microtubules in S2 cells and mitochondria in HeLa cells.**

Fluorescence microscopy is widely used in biology because of its ability to study the three-dimensional (3D) interior of living cells and to visualize molecules of interest with great specificity through fluorescence labeling. Unfortunately its spatial resolution is fundamentally limited by diffraction to about 200 nm and 600 nm in the lateral and axial directions, respectively. Several methods have been reported in recent years<sup>1–3</sup> that can achieve resolution well below these limits, but each technique imposes its own constraints that can limit its capability to rapidly image 3D samples, the ultimate goal of any imaging technique.

Localization-based super-resolution methods such as photo-activated localization microscopy (called PALM)<sup>2</sup> and stochastic optical reconstruction microscopy (STORM)<sup>3</sup> have achieved 20-nm lateral resolution by precisely localizing individual photo-activatable fluorophores but require hundreds to tens of thousands of exposures and are therefore limited in speed. Although it has been demonstrated that localization precision can be extended to the axial dimension<sup>4–6</sup> and applied to fixed whole-cell imaging<sup>7,8</sup>, live-cell applications of localization-based super-resolution techniques have so far been limited to two dimensions<sup>9,10</sup> or thin-layered 3D microscopy<sup>11</sup> presumably because the speed of these techniques is insufficient for imaging thicker volumes. Thin-layered 3D live STORM<sup>11</sup> achieved an impressive 0.5–1 Hz 3D frame rate but produced only six frames owing to the high light intensity (15 kW cm<sup>-2</sup>) needed for such a high rate.

Stimulated emission depletion (STED) microscopy is another resolution-enhancing technique based on suppressing the periphery of the illuminated spot through stimulated emission<sup>1</sup>. The speed of STED microscopy, a point-scanning method, is fundamentally limited by its scanning mechanism and the size of the area to be scanned, especially as the resolution increases. To reach a biologically useful speed in STED microscopy, each pixel is left with a dwell time of merely tens of microseconds, and thus excitation intensity of 0.04–6 MW cm<sup>-2</sup> is needed to record sufficient photons<sup>12</sup>. In addition, the resolution of STED microscopy scales as the inverse square root of the stimulated emission beam's intensity<sup>1</sup> and 38–540 MW cm<sup>-2</sup> of such intensity is needed to achieve a 65-nm lateral resolution<sup>12</sup>. Therefore photodamage and photobleaching may also be major limiting factors and concerns for live-cell STED microscopy. STED microscopy has been applied to fast live imaging<sup>1,12</sup>, but has been confined to two dimensions and relatively small fields of view of ~4.5 μm<sup>2</sup>. Given these drawbacks, there is still a need for a technique that can produce time-lapse 3D images of live whole cells over at least tens of time points at subdiffraction-limited resolution.

Three-dimensional structured-illumination microscopy (SIM) is a wide-field technique that achieves lateral and axial resolution of 100 nm and 300 nm, respectively<sup>13</sup>, using spatially structured illumination light. The patterned illumination moves high-resolution sample information into the normal pass-band of the microscope through frequency mixing, resulting in a doubling of both the lateral and axial resolution and true optical sectioning, that is, rejection of out-of-focus blur, a major weakness in conventional 3D wide-field microscopy. Whereas the enhanced resolution of 3D SIM is not as high as that of the above methods, 3D SIM is potentially faster because it requires much fewer raw images than PALM or STORM and is not a point-scanning method such as STED microscopy. SIM has been implemented on fixed cells in three dimensions<sup>13</sup> and living cells in two dimensions<sup>14,15</sup>, but to our knowledge has never been applied to 3D volumetric imaging of a living cell. Here we demonstrate whole-cell live 3D SIM on two types of living samples over tens to hundreds of time points at 120-nm lateral and 360-nm axial spatial resolution, and 5–25 s per volume temporal resolution using low light intensities of ~5 W cm<sup>-2</sup>.

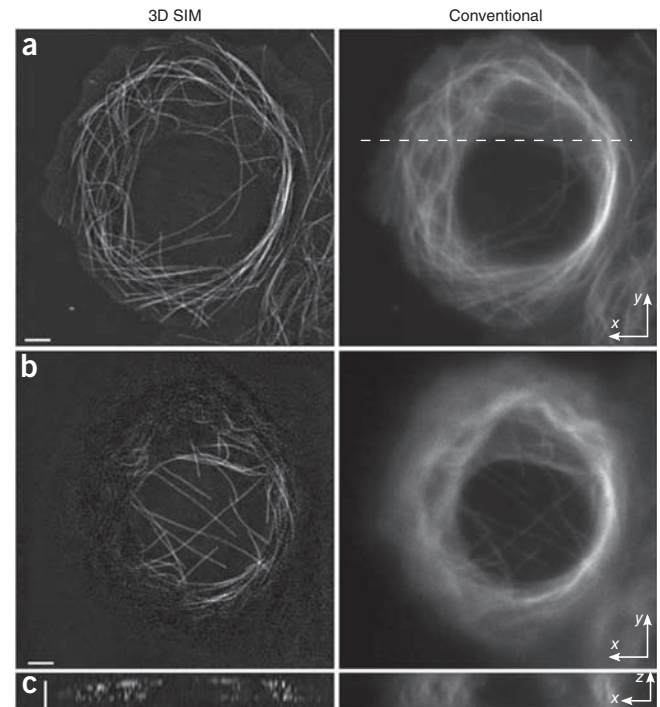
In our original implementation of 3D SIM<sup>13</sup>, we had placed a transmission phase grating in the illumination path to diffract a collimated beam into three illumination beams that were then directed onto the sample. The interference of these three beams results in a spatially structured illumination pattern in three dimensions that is used for resolution enhancement. For each axial plane of a 3D stack, 15 exposures with 15 different patterns

<sup>1</sup>Janelia Farm Research Campus, Howard Hughes Medical Institute, Ashburn, Virginia, USA. <sup>2</sup>Faculty of Engineering, University of Georgia, Athens, Georgia, USA.

<sup>3</sup>Graduate Program in Biophysics, University of California, San Francisco, San Francisco, California, USA. <sup>4</sup>Deceased. Correspondence should be addressed to L.S. (shaol@janelia.hhmi.org).

**Figure 1** | Live 3D SIM and conventional wide-field microscopy images of a *Drosophila* S2 cell expressing  $\alpha$ -tubulin-EGFP. (a,b) Two x-y planes at  $z = 0.16 \mu\text{m}$  (a) and  $z = 2.24 \mu\text{m}$  (b) of the 3D volume at time 0 of 150 time points. Each SIM volume was acquired in 5.04 s (that is, 18-ms exposure time  $\times$  18 axial planes  $\times$  15 patterns + 18 axial planes  $\times$  10-ms z-stage settle time). (c) A single x-z cross-section cut through the dashed line shown in a. All scale bars,  $2 \mu\text{m}$ .

are needed: three lateral orientations rotationally spaced at  $60^\circ$  and five different phases in each orientation. The speed-limiting step in data acquisition is the time to mechanically rotate ( $\sim 1$  s) and translate ( $\sim 10$  ms) the grating for all the pattern orientations and phases, respectively. These factors mean that the acquisition speed is simply not high enough for live-cell imaging. Recently we had reported using a ferroelectric liquid crystal spatial light modulator (SLM) to produce the patterns for live 2D SIM in total internal reflection fluorescence (TIRF) mode<sup>13</sup>, which achieves 100-nm lateral resolution at up to 11 Hz for several hundred time points. Key to the drastic speed improvement had been the sub-millisecond pattern switching time provided by the SLM. Here we used a system similar to that of the live TIRF-SIM for live 3D SIM (Supplementary Fig. 1) with several modifications: we used a water-immersion  $60\times$  objective lens and different SLM patterns (Supplementary Fig. 2), and we unblocked the 0 diffraction order to obtain an axial component to the illumination pattern. As the SLM allowed the pattern to be switched between orientations and phases on a much faster time scale, the image acquisition time was limited by the camera readout time or the exposure time if that was longer. In addition, because there was no difference between the time needed for pattern rotation and translation, we acquired all 15 images in each axial plane first before switching to the next plane, unlike the imaging sequence in the originally reported 3D SIM<sup>13</sup>. This new imaging sequence



was more compatible for live 3D imaging as spatially connected parts in the raw data were also temporally connected.

To test 3D SIM for live imaging, we first imaged *Drosophila melanogaster* S2 cells stably expressing  $\alpha$ -tubulin genetically fused to enhanced GFP (EGFP). Compared to conventional wide-field microscopy, SIM improved both lateral and axial resolution (Fig. 1), and rejected out-of-focus light resulting in true optical sectioning. We compared Fourier transforms of the 3D SIM images and conventional wide-field images of this dataset (Supplementary Fig. 3). To make the S2 cells adhere to the cover glass, we covered the S2 cells using a thin layer of agarose gel, resulting in cell thickness of  $2.5\text{--}3.5 \mu\text{m}$ . We scanned the sample through focus using a step size of  $0.16 \mu\text{m}$ , slightly smaller than the Nyquist sampling requirement. The lateral size of the S2 cells covered with gel was about  $25 \times 25 \mu\text{m}^2$  (Fig. 1) and could

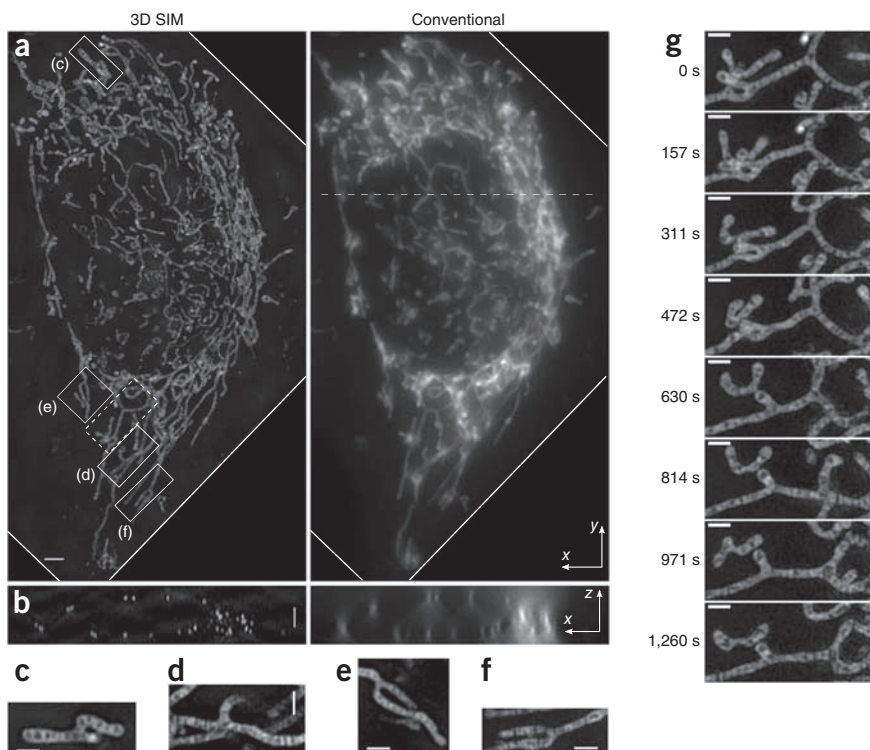


**Figure 2** | Live 3D SIM and conventional wide-field microscopy images of a HeLa cell stained with MitoTracker Green. (a) Maximum-intensity projection along z dimension through the cell volume at time 0 of a 50-time-point series. Each SIM volume was acquired in 20.33 s (that is, 35-ms exposure time  $\times$  38 axial planes  $\times$  15 patterns + 38 axial planes  $\times$  10-ms z-stage settle time). (b) One x-z cross-section of the same volume sliced through the dashed line shown in a. (c-f) Single-plane x-y slices corresponding to the boxed regions in a. (g) Eight time frames of the region boxed with dashed line in a. Each frame is a maximum-intensity projection along z over a  $1.3 \mu\text{m}$  thickness that contains the featured Y-shaped mitochondrion. Scale bars,  $2 \mu\text{m}$  (a,b) and  $1 \mu\text{m}$  (c-g).

be captured by  $256 \times 256$  camera pixels, which took about 18 ms per exposure on our electron-multiplying charge-coupled device (EMCCD). Thus for a single S2 cell, about 5 s were needed to acquire all raw images for one 3D SIM volume. As demonstrated by a movie of the time-lapse series (**Supplementary Video 1**), this imaging speed was sufficient to capture highly dynamic microtubule polymerization and depolymerization and overall movements without visible motion artifacts. This series spanned 150 time points and used 40,500 exposures in total, yet because of the low photobleaching rate, the signal-to-noise ratio was sufficient even at the end of the series. We suspect that the low illumination intensity of  $5.5 \text{ W cm}^{-2}$  we needed was partly responsible for the slow photobleaching.

We next imaged mitochondria dynamics in living HeLa cells stained with MitoTracker Green, a mitochondria-specific fluorescent dye (**Fig. 2** and **Supplementary Videos 2–6**). Again, 3D SIM images demonstrate much improved lateral (**Fig. 2a** and **Supplementary Fig. 4**) and axial (**Fig. 2b**) resolution over conventional wide-field microscopy. Whereas deconvolution could remove the out-of-focus background in the conventional wide-field images (**Supplementary Fig. 5**), it provided little resolution enhancement. Imaging HeLa cells was more challenging because their size is much bigger both laterally ( $40\text{--}60 \mu\text{m}$ ) and axially ( $6\text{--}8 \mu\text{m}$ ) than that of S2 cells. The full EMCCD chip ( $512 \times 512$  pixels) and  $\sim 40$  axial planes were typically needed to capture movement throughout an entire HeLa cell. Using 35 ms per exposure, we acquired one SIM volume in 21 s. Even with such modest speed, the occurrences of motion artifacts were rare (for example, **Supplementary Video 7**). We acquired 50 time points over 25 min (**Fig. 2** and **Supplementary Videos 2** and **3**) and 75 time points over 37 min (**Supplementary Video 6**) without substantial photobleaching. These series captured mitochondria movements of up to  $0.12 \mu\text{m s}^{-1}$  and fission-fusion events (**Supplementary Videos 2–6**). The measured speed was slightly lower than the previously reported speed<sup>16</sup> presumably because we imaged at room temperature (Online Methods). Furthermore, fine structures in mitochondria that resemble the cristae seen usually only in electron micrographs were clearly visible (**Fig. 2c–g**). These internal mitochondrial structures appeared highly dynamic over time under live 3D SIM (**Fig. 2g** and **Supplementary Videos 4** and **5**).

It is critical in live microscopy that the imaging time be short enough so that sample movement during acquisition is less than one resolution length. With 21 s per volume imaging time for the HeLa cell dataset, this speed requirement was obviously unmet, and yet we rarely saw motion artifacts. This can be explained by taking into account the shallow depth of focus in high-numerical-aperture 3D microscopy. Our calculations show that (**Supplementary Fig. 6**) the depth of focus under 3D SIM is  $0.4 \mu\text{m}$ , which suggests that any fluorophore more than  $0.2 \mu\text{m}$  away from the focal plane will have minimal impact to the rest of the 3D volume. Consequently, the motion tolerance in 3D SIM can be relaxed to one resolution length per amount of time needed for focus-scanning through a thickness of  $0.4 \mu\text{m}$ , which translates to between  $183 \text{ nm s}^{-1}$  ( $256 \times 256$  pixels) and  $91 \text{ nm s}^{-1}$  ( $512 \times 512$  pixels). Our simulation results confirmed that under the

same imaging conditions as used for the HeLa cell dataset, an object moving at  $100 \text{ nm s}^{-1}$  is well tolerated by live 3D SIM (**Supplementary Fig. 7**).

In summary, we demonstrated SLM-based 3D SIM as a useful tool for live-cell imaging with a spatial resolution twice that of conventional microscopy and a moderate temporal resolution that is limited by the camera readout time. A temporal resolution ten times as high as reported here is possible with emerging technologies such as scientific complementary metal–oxide–semiconductor cameras. To our knowledge, SIM is currently the only super-resolution technique capable of time-lapse whole-cell 3D imaging over tens to hundreds of time points. Notably, it does not require special fluorescent probes or extreme light intensities and is readily extensible to multicolor imaging as demonstrated earlier in fixed-cell SIM<sup>13</sup> (**Supplementary Note**).

## METHODS

Methods and any associated references are available in the online version of the paper at <http://www.nature.com/naturemethods/>.

*Note: Supplementary information is available on the Nature Methods website.*

## ACKNOWLEDGMENTS

We dedicate this paper to the late Dr. Mats Gustafsson. We thank H. White and A. Arnold for assistance with sample preparation; S. Goodwin, S.A. Ribeiro and R. Vale (University of California, San Francisco), for providing the S2 cells; R. Fiolka and E. Betzig for valuable discussions, and L. Winoto for sharing the design of the optical fiber shaker.

## AUTHOR CONTRIBUTIONS

L.S. and P.K. built the optical hardware and wrote the software for the control system and image acquisition. P.K. built the electronics circuit that interfaces the digital signal processing board with the rest of the system. L.S. prepared the samples, and acquired and processed data. E.H.R. provided guidance on biological applications. M.G.L.G. made the conceptual design. L.S. and E.H.R. wrote the manuscript.

## COMPETING FINANCIAL INTERESTS

The authors declare no competing financial interests.

Published online at <http://www.nature.com/naturemethods/>.

Reprints and permissions information is available online at <http://www.nature.com/reprints/index.html>.

- Westphal, V. *et al. Science* **320**, 246–249 (2008).
- Betzig, E. *et al. Science* **313**, 1642–1645 (2006).
- Rust, M.J., Bates, M. & Zhuang, X. *Nat. Methods* **3**, 793–795 (2006).
- Huang, B., Wang, W., Bates, M. & Zhuang, X. *Science* **319**, 810–813 (2008).
- Juette, M.F. *et al. Nat. Methods* **5**, 527–529 (2008).
- Shtengel, G. *et al. Proc. Natl. Acad. Sci. USA* **106**, 3125–3130 (2009).
- Huang, B., Jones, S.A., Brandenburg, B. & Zhuang, X. *Nat. Methods* **5**, 1047–1052 (2008).
- York, A.G., Ghitani, A., Vaziri, A., Davidson, M.W. & Shroff, H. *Nat. Methods* **8**, 327–333 (2011).
- Shroff, H., Galbraith, C.G., Galbraith, J.A. & Betzig, E. *Nat. Methods* **5**, 417–423 (2008).
- Wombacher, R. *et al. Nat. Methods* **7**, 717–719 (2010).
- Jones, S.A., Shim, S., He, J. & Zhuang, X. *Nat. Methods* **8**, 499–508 (2011).
- Lauterbach, M.A. *et al. J. Biophoton.* **3**, 417–424 (2010).
- Gustafsson, M.G.L. *et al. Biophys. J.* **94**, 4957–4970 (2008).
- Kner, P., Chhun, B.B., Griffis, E.R., Winoto, L. & Gustafsson, M.G. *Nat. Methods* **6**, 339–342 (2009).
- Hirvonen, L.M., Wicker, K., Mandula, O. & Heintzmann, R. *Eur. Biophys. J.* **38**, 807–812 (2009).
- Bereiter-Hahn, J. & Jendrach, M. *Int. Rev. Cell Mol. Biol.* **284**, 1–65 (2010).







## ONLINE METHODS

**Cell maintenance and preparation.** *Drosophila* S2 cells stably expressing *EGFP- $\alpha$ -tubulin* under the control of the *Ac5* promoter were maintained as described previously<sup>17</sup>. The cells were suspended in their conditioned medium to a concentration of  $2 \times 10^7$  cells ml<sup>-1</sup>, and 25  $\mu$ l of this suspension was pipetted onto a cleaned 22 mm  $\times$  22 mm #1.5 coverslip and covered with a piece of 170- $\mu$ m-thick 2% agarose gel, as described previously<sup>18</sup> except omitting the spacers. The agarose pad was covered with a round coverslip of 18 mm diameter and sealed with valap. Samples were imaged through the 22 mm  $\times$  22 mm coverslip.

HeLa cells were grown on cleaned 22 mm  $\times$  22 mm #1.5 coverslips and stained in 50 nM MitroTracker Green FM (Invitrogen) solution in growth medium for 30 min inside a 37 °C incubator. The growth medium was then replaced with a HEPES-based buffer (75 mM NaCl, 10 mM HEPES, 0.5 mM CaCl<sub>2</sub>, 2.5 mM KCl and 0.5 mM MgCl<sub>2</sub>; pH 7.4) used as the mounting medium. The coverslip was then removed from the incubator, covered with a small round coverslip and sealed as described above. Samples were imaged at room temperature (24 °C) through the 22 mm  $\times$  22 mm coverslip within 30 min after being removed from the incubator.

**Structured illumination.** Excitation light (488 nm; Sapphire 488-500 CDRH; Coherent) was coupled via an acousto-optic deflector (AOM-40 AF; Intra-action) into a multimode optical fiber (core size, 100  $\mu$ m; numerical aperture (NA) 0.12; CeramOptec). The acousto-optic deflector was used as a fast shutter and intensity control. The fiber was mounted on a high-frequency mechanical shaker, composed of two eccentrically loaded brushless direct-current motors (1935 006 BRE; Faulhaber) mounted in parallel but oppositely in a Delrin block, which was suspended by four springs in a star-like formation, to produce a rapidly time-varying speckle pattern at the fiber output; over typical exposure times, the speckle pattern averaged out to an approximately constant intensity, producing a simulated spatially incoherent light source at the fiber output (**Supplementary Discussion** and **Supplementary Video 8** contain details on the uniformity of the illumination light thus generated). The light exiting the fiber was collimated and sent through a pattern generator (**Supplementary Fig. 1**) consisting of a 1,024  $\times$  768 pixel ferroelectric liquid crystal on silicon SLM (Micron), a polarizing beam splitter cube and a half-wave plate. These three components worked together as a binary phase modulator, with each SLM pixel producing a phase shift of nominally zero radians in its off state or  $\pi$  radians in its on state<sup>14</sup> (**Supplementary Table 1**). The light exiting the pattern generator was thus diffracted and directed toward the microscope through a polarization rotator (**Supplementary Fig. 1** and **Supplementary Table 2**) consisting of two custom ferroelectric liquid crystal phase retarders with one-third-wave retardance (Micron) and a quarter-wave plate. The purpose of the polarization rotator was to maintain the s-polarization of the illumination light for each of the three pattern orientations so that the illumination pattern has maximal contrast in the sample<sup>14</sup>. Unwanted diffraction orders, caused by the finite-sized pixels of the SLM<sup>14</sup>, were blocked by a mask located in a pupil plane. The desired 0 and  $\pm 1$  diffraction orders were refocused to the center and two points near the opposite edges of the back focal plane of the microscope objective,

respectively. After being recollimated by the objective lens (Plan Apo VC 60 $\times$  WI, NA 1.2; Nikon), all three beams approached the sample and interfered to produce a 3D pattern of excitation intensity<sup>13</sup>. Fluorescent emission light from the specimen was collected by the same objective and directed toward a camera by a dichromatic beam splitter, as in a conventional fluorescence microscope. The dichromatic beam splitter (ZT405/488/561 TPC-22.5deg; Chroma) used a custom coating with minimal transmission retardance at the excitation wavelength to maintain the desired polarization state of the illumination beams, was deposited on a 3.2-mm-thick optically flat substrate to minimize aberrations in the reflected emission light and was operated at 22.5° to minimize aberrations in the transmitted excitation light.

Fifteen SLM patterns were prepared, each corresponding to a particular orientation-phase combination. The  $\pm 60^\circ$  patterns were similar to those used in 2D TIRF SIM<sup>14</sup> (**Supplementary Fig. 2**), except for the 30% duty cycle for producing the zero diffraction order that is essential for 3D SIM and a 10-pixel horizontal period so as to allow exact  $2\pi/5$  phase shifts. For the 0° orientation, a horizontal pattern of 5-pixel period was used. To meet the 30% duty cycle requirement, vertically interleaving 20% and 40% duty cycles had to be used because it is impossible to directly generate 30% duty cycle with the 5-pixel period. One side effect of such interleaving patterns is the generation of vertical diffraction orders; but because of the small vertical period (2 pixels), all nonzero vertical diffraction orders are easily blocked by the pupil mask.

The ferroelectric liquid crystal SLM was driven with a direct current electric field, with opposite directions for the on and off pixel states; this field must time-average to zero to avoid slow deterioration of the device through charge migration. Each pixel must thus spend equal time on and off. To this end, each pattern was polarity-switched (switching on pixels to off and vice versa) halfway through each exposure. The illumination light was shuttered off while a new pattern was being written to the SLM. The two polarities produce different order-zero diffraction strength except when the fast axis of the half-wave plate in the pattern generator is exactly rotated 11.25° (or  $\pi/16$  radians) from the horizontal axis (**Supplementary Fig. 8**), which is also the desired position of maximal  $\pm 1$  diffraction orders' intensity. We precisely located this angular position of the half-wave plate by minimizing the zero-order intensity difference between the two pattern polarities.

**Acquisition.** All 15 pixel patterns were preloaded onto the SLM controller circuit board. Axial position of the sample is controlled by a piezoelectric translational stage (P-753 LISA; Physik Instrumente). Images were acquired at 24 °C. At each time point, raw SIM data were acquired for each axial plane at five phases spaced by  $2\pi/5$  for each of the three pattern orientations before the axial stage moved to the next plane. This sequence differs from the originally reported 3D SIM<sup>13</sup> in which all planes in one pattern orientation were acquired first before switching to the next orientation. The back-illuminated EMCCD camera (iXon+, DU-897E-CS0-#BV; Andor) was operated in externally triggered frame-transfer mode at -78 °C with liquid cooling and read out at 10 MHz with 14-bit analog-to-digital conversion. The acousto-optical shutter opening and closing, SLM pattern loading and polarity switching, trigger for the camera to initiate frame transfer,

trigger for the polarization rotators to rotate the fast axes and axial stage positioning were all precisely synchronized by a timed interrupts-based program running on a digital signal processing board (M67; Innovative Integration).

**Data processing.** The time-lapse 3D SIM data were first background-corrected and then intensity-equalized over each volume and over all the time points. The 3D SIM volume at each time point was then independently reconstructed using a generalized Wiener filter as described previously<sup>13,14</sup>, implemented in the C programming language. To obtain the conventional wide-field images for comparison purpose (Figs. 1 and 2), we simply averaged the raw images over the five pattern phases within the first SIM pattern angle.

One crucial parameter in the Wiener filter is the Wiener parameter that appears in the denominator<sup>13</sup> as a means for preventing noise artifacts in the filtering result. This parameter should in theory be set to the inverse of signal-to-noise ratio in the raw data but instead was empirically set to the value that visually provides the best trade-off between resolution and noise artifacts. In time-lapse microscopy in general, signal-to-noise ratio decreases over time because of photobleaching, and the Wiener parameter used in SIM reconstruction should increase accordingly. In this work both of the following methods were used: a constant Wiener parameter throughout the time series (Figs. 1,2 and **Supplementary Videos 1–5**) and linearly increasing Wiener parameter over the time points (**Supplementary Video 6**).

**Figure preparation.** Raw and reconstructed SIM images were saved in MRC format, originally devised for X-ray crystallography and electron microscopy at the MRC Laboratory of Molecular Biology. Image analysis and rendering were done using Priism

software package (<http://msg.ucsf.edu/IVE/>). To prepare the figures that contain images, the MRC images were first converted to 8-bit TIFF format using Priism and then assembled into figures using Inkscape or Adobe Illustrator. All real-space images except for those shown in **Supplementary Figure 4** were shown in gray-scale with gray levels linearly mapped between the background mean and the peak intensity of each image. All figures were prepared with Inkscape except for those shown in **Supplementary Figures 1 and 4**, which were prepared with Adobe Illustrator.

To encode depth information in colors in **Supplementary Figure 4**, three copies of the same 3D stack were made, with each used for one color channel. The red-channel stack was multiplied by a downward-opening parabolic function of  $z$  increasing from 0 to 1 between shallow and deep  $z$  positions, the green-channel stack by a downward-opening parabolic function of  $z$  decreasing from 1 to 0 and the blue-channel stack by an upward-opening parabolic function with 0 at the middle point and 1 at the two ends of the  $z$  range. The three stacks were then maximum intensity-projected separately and merged to form the colored images using Priism.

The supplementary videos were created using QuickTime Pro (Apple) with MPEG-4 encoding from a series of 8-bit TIFF images, converted from MRC by Priism. To satisfy file size requirement, **Supplementary Videos 1 and 6** were shrunk from the original size by a factor of 1.14 and 1.62, respectively, but with the increased resolution still appreciable.

17. Rogers, S.L., Rogers, G.C., Sharp, D.J. & Vale, R.D. *J. Cell Biol.* **158**, 873–884 (2002).
18. Maiato, H., Rieder, C.L. & Khodjakov, A. *J. Cell Biol.* **167**, 831–840 (2004).

Reproduced with permission of the copyright owner. Further reproduction prohibited without permission.